Supplementary Material

Hepatic PPARα is critical in the metabolic adaptation to sepsis

Réjane PAUMELLE, Joel HAAS, Nathalie HENNUYER, Eric BAUGE, Yann DELEYE, Dieter MESOTTEN, Lies LANGOUCHE, Jonathan VANHOUTTE, Céline CUDEJKO, Kristiaan WOUTERS, Sarah Anissa HANNOU, Vanessa LEGRY, Steve LANCEL, Fanny LALLOYER, Arnaud POLIZZI, Sarra SMATI, Pierre GOURDY, Emmanuelle VALLEZ, Emmanuel BOUCHAERT, Bruno DERUDAS, Hélène DEHONDT, Céline GHEERAERT, Sébastien FLEURY, Anne TAILLEUX, Alexandra MONTAGNER, Walter WAHLI, Greet VAN DEN BERGHE, Hervé GUILLOU, David DOMBROWICZ and Bart STAELS.

Table of contents

Supplementary Methods

Bone marrow transplantation

10 week-old female C57BL/6J *Pparα* WT and KO mice were lethally irradiated (8 Gy) and tail vein injected the next day with $5x10^6$ bone marrow cells isolated from 10 week-old female *Pparα* WT donor mice. Mice received autoclaved acidified water (pH=2) supplemented with neomycin 100 mg/L (Cat.N1142, Sigma-Aldrich) and polymyxin B sulphate 60000 U/L (Cat.21850029, Invitrogen) 1 week before and 4 weeks after transplantation. Mice were studied 8 weeks post-transplantation allowing complete repopulation by the donor bone marrow. To ensure that donor bone marrow efficiently replaced the resident blood cell population, DNA was extracted from whole blood with an Illustra blood kit (GE Healthcare). PCR was performed with the forward 5'-cggcctggccttctaaac-3' and reverse 5'-agcgctgcgtcggact-3' primers, yielding products of different lengths depending on the genotype, separated on a 1.5% agarose gel and quantified with the Gel Doc XR system (Bio-Rad). Over 95% of host blood cells were from donor origin. Circulating immune cell composition was found to be similar between the genotypes (data not shown).

Characterization of hepatocyte-specific Pparα-deficient mice

Hepatocyte-specific *Pparα* deletion was confirmed on mRNA isolated from livers by PCR using HotStar Taq DNA Polymerase (5 U/µL, Qiagen) and forward (Lf; 5′-AAAGCAGCCAGCTCTGTGTTGAGC-3′) and reverse primers (Er; 5′-TAGGTACCGTGGACTCAGAGCTAG-3′) [1]. Amplification conditions were as

follows: 95°C for 15 min; followed by 35 cycles of 94°C for 1 min, 65°C for 1 min, and 72°C for 1 min; and 72°C for 10 min. This reaction produced 450, 915, and 1070 bp fragments for the exon 4 deletion, the wild-type and the floxed alleles, respectively. The albumin-Cre allele was detected by PCR using the following primer pairs: CreU (5′-AGGTGTAGAGAAGGCACTTAG-3 and CreD (5′-CTAATCGCCATCTTCCAGCAGG-3′), and G2lox7F (5′-CCAATCCCTTGGTTCATGGTTGC-3′) and G2lox7R (5′-CGTAAGGCCCAAGGAAGTCCTGC-3′). *Ppara*^{hepWT} (Albumin-Cre^{-}, *Ppara fl/fl*) littermate mice were used as controls.

RNA analysis

Mouse tissue RNA extraction was performed using TRIzol reagent and reverse transcription was performed according to the manufacturer's protocol (Invitrogen Life technologies). RNA levels were measured by quantitative PCR using brilliant SYBR Green QPCR Master Mix on the MX4000 detection system (Stratagene). The amplifying murine primers (Eurogentech) are indicated in supplementary CTAT table. Cycle threshold (Ct) values were determined for target genes and normalized to the Ct of cyclophilin using the following equation: relative values = 2^–(Ct target gene- Ct cyclophilin). Results are expressed as means ± SEM (n=8).

Human liver RNA analysis

RNA was isolated from livers using the RNeasy mini RNA isolation kit (Qiagen, Hilden, Germany) and quantified by Nanodrop spectrophotometry (ND-1000, Nanodrop Technologies). Reverse transcription was performed according to the manufacturer's protocol (Invitrogen Life technologies). RNA levels of the tested genes were measured by quantitative real time PCR with commercial TaqMan chemistry gene expression assays (Life Technologies) as indicated in supplementary CTAT table and StepOnePlus sequence detector (Life Technologies). Cycle threshold (Ct) values were determined for target genes and normalized to the Ct of Glyceraldehyde 3-phosphate dehydrogenase. Data are expressed as fold increase relative to the mean of the control patients. Results are expressed as means ± SEM.

Citrate synthase activity

Citrate synthase (CS) activity was measured on liver homogenates using Oroboros technology. Briefly, in a 96-well plate, 2µg of liver homogenate proteins were added in CS buffer (20mM Trizma Base, 1,25mM EDTA, pH8), in presence of acetyl-coA, DTNB and oxaloacetic acid. Absorbance at 412 nm was measured for 2 min, every 20 seconds. The slope was calculated and CS activity was obtained using following the equation: (slope/13600)*(1/µg proteins)*10^9.

Hepatic triglyceride measurement

Hepatic triglyceride (TG) content was measured essentially as described [1,3]. Briefly, 50-100 mg of liver tissue was homogenized in 1 mL of PBS. 200 µL of the homogenate was used for extraction with 3 ml of 2:1 chloroform:methanol. After addition of 300 µL H_2O and phase separation, the upper aqueous phase was discarded and 1 mL of 1% Triton-X100 in chloroform was added to the remaining organic phase. The organic phase was evaporated to dryness and the detergent pellet was resuspended in 200 µL ddH_2O. TG concentrations in the solution were quantified by colorimetric assay (Diasys).

Western blot analysis

Liver samples (~30 mg) were homogenized using a polytron in 1 mL ice cold RIPA buffer supplemented with PMSF, sodium fluoride, and sodium orthovanadate. Samples were mixed continuously by inversion in a rotating agitator at 4°C for 1 hour, then centrifuged at 13000 x g for 10 min at 4°C to pellet insoluble material. Supernatants were removed and the protein concentration was equalized by dilution with additional RIPA buffer. Soluble protein was quantified by BCA assay (Interchim, France), and equal protein amounts from two mouse livers were pooled per lane. Proteins were separated by SDS-PAGE and transferred to nitrocellulose membranes according to standard protocols. Primary antibodies were incubated overnight in 5% non-fat milk diluted in Tris-buffered saline, 0.1% Tween-20 (TBST) at 4°C.

Fluorescent or HRP-conjugated secondary antibodies were incubated for 1 hour at room temperature. Antibody references are indicated in CTAT methods.

CTAT Methods

1.1 Antibodies

Name	**Citation**	**Supplier**	**Cat no.**	**Clone no.**
HMGCS2		Santa Cruz	sc-376092	(G-11)
DGAT1	Camus, et al, JBC 2013	Santa Cruz	sc-32861	(H-255)
ATGL		Cell Signal	2439S	(30A4)
Ulk1	Lancel, et al. JCI Insight 2018	Abcam	ab128859	
Atg5	Lancel, et al. JCI Insight 2018	Novus	NB110-53818	
LC3B	Lancel, et al. JCI Insight 2018	Abcam	ab51520	
HSP90		Santa Cruz	sc-7947	(H-114)
Moma2		Abcam	ab33451	GR316059-17
Ly6G		BD Pharmingen	551459	1A8

1.2 Organisms

Name	**Citation**	**Supplier**	**Strain**	**Sex**	**Age**	**Overall n number**
Ppara WT and Ppara KO littermates	Lee SS, et al. MCB 1995	Internal breeding established from F. Gonzalez (NIH,	C57BL6/J background	Females	12-14 wks	n = 81

		Bethesda, USA)				
Ppara fl/fl, Alb-Cre (hepatocyte-specific Ppara-KO)	Montagner A, et al. Gut 2016	Internal Breeding from H. Guillou (INRA, Toulouse, France)	C57BL6/J background	Females	12-14 weeks	n = 95

1.3 Sequence based reagents

Name	**Sequence**	**Supplier**
Cyclophillin-F	GCATACGGGTCCTGGCATCTTGTCC	Eurogentec
Cyclophillin-R	ATGGTGATCTTCTTGCTGGTCTTGC	Eurogentec
Ulk1-F	GAG CCG AGA GTG GGG CTT TGC	Eurogentec
Ulk1-R	GCC CTG GCA GGA TAC CAC GC	Eurogentec
Bnip3-F	GCTCCTGGGTAGAACTGCAC	Eurogentec
Bnip3-R	GCTGGGCATCCAACAGTATT	Eurogentec
Atg5-F	AGCAGCTCTGGATGGGACTGC	Eurogentec
Atg5-R	GCCGCTCCGTCGTGGTCTGA	Eurogentec
Beclin1-F	CCGGGCGATGGGAACTCTGGA	Eurogentec
Beclin1-R	CCTCCATGCCTCAGGAGCCCG	Eurogentec
Tnfa-F	CCCCAAAGGGATGAGAAGTT	Eurogentec
Tnfa-R	CACTTGGTGGTTTGCTACGA	Eurogentec
Mcp1-F	GCCAACTCTCACTGAAGCC	Eurogentec
Mcp1-R	GCTGGTGAATGAGTAGCAGC	Eurogentec
Il6-F	AACGATGATGCACTTGCAGA	Eurogentec
Il6-R	GGTACTCCAGAAGACCAGAGGA	Eurogentec
Ifng-F	GCTTTGCAGCTCTTCCTCAT	Eurogentec

Ifng-R	TTTTGCCAGTTCCTCCAGAT	Eurogentec
Vcam1-F	AACCGAATCCCCAACTTGTGCAG	Eurogentec
Vcam1-R	TCTCCAGCTTCTCTCAGGAAATGCC	Eurogentec
Icam1-F	CCTGGCCTCGGAGACATTAGAGAAC	Eurogentec
Icam1-R	ACCCCAAGGAGATCACATTCACGG	Eurogentec
Sod2-F	CACATTAACGCGCAGATCATG	Eurogentec
Sod2-R	CCAGAGCCTCGTGGTACTTCTC	Eurogentec
Pepck1-F	AGCCTCGACAGCCTGCCCCAGG	Eurogentec
Pepck1-R	CCAGTTGTTGACCAAAGGCTTTT	Eurogentec
Fbp1-F	TCCTACGCTACCTGTGTTCTTG	Eurogentec
Fbp1-R	GGCAGTCAATGTTGGATGAG	Eurogentec
Pdk4-F	TCCTTCACACCTTCACCACA	Eurogentec
Pdk4-R	TCTTCTTTTCCCAAGACGACA	Eurogentec
Ppara-F	ATCGCGTACGGCAATGGCTTTA	Eurogentec
Ppara-R	CAGGCCGATCTCCACAGCAAATTA	Eurogentec
Cd36-F	GCACCACTGTGTACAGACAG	Eurogentec
Cd36-R	GTGCAGCTGCTACAGCCAG	Eurogentec
Fatp1-F	GATGTGCTCTATGACTGCCTG	Eurogentec
Fatp1-R	GTGTCGCTGCTCCACGTCG	Eurogentec
Acsl1-F	CGCTCTGTCACACACTTCGA	Eurogentec
Acsl1-R	CTACAGCTTCTCTGCCAAGTGTG	Eurogentec
Cpt1a-F	CATCATGACTATGCGCTACTC	Eurogentec

Cpt1a-R	CAGTGCTGTCATGCGTTGG	Eurogentec
Acox1-F	ACATCTTGGATGGTAGTCCG	Eurogentec
Acox1-R	TAACGCTGGCTTCGAGTGAG	Eurogentec
Lcad-F	ATCTTTTCCTCGGAGCATGA	Eurogentec
Lcad-R	TTTCTCTGCGATGTTGATGC	Eurogentec
Hmgcs2-F	TGGTGGATGGGAAGCTGTCTA	Eurogentec
Hmgcs2-R	TTCTTGCGGTAGGCTGCATAG	Eurogentec
Atgl-F	CCACATTGGCGTGGCCTCCT	Eurogentec
Atgl-R	AACCGCTTCCGGGCCTCCTT	Eurogentec
PPARa	Hs00947536	Life technology
ATGL	Hs00982043	Life technology
PDK4	Hs01037712	Life technology
CD36	Hs01567185	Life technology
HMGCS2	Hs00985427	Life technology
LCAD	Hs01085277	Life technology

1.4 Biological samples

Description	**Source**	**Identifier**
Escherichia Coli DH5α	Thermo Fischer	18265-017

1.5 Deposited data

Name of repository	**Identifier**	**Link**
Gene Expression	GSE121847	https://www.ncbi.nlm.nih.gov/geo/query/acc.cgi?acc=GSE121847

Omnibus (microarray data)		

1.6 Software

Software name	**Manufacturer**	**Version**
R	R-project (open source)	x64 3.5.0
oligo	Bioconductor (open source)	1.44.0
clusterProfiler	Bioconductor (open source)	3.8.1
Partek genomic suite	Partek	7.0
Graph Pad	Prism	5.01
NIS Elements	Nikon	BR 4.20.03 (build 995)

1.7 Please provide the details of the corresponding methods author for the manuscript:

Joel Haas**,** Univ. Lille, Inserm, CHU Lille, Institut Pasteur de Lille, U1011, EGID, F, 59000 Lille, France. joel.haas@pasteur-lille.fr

1.8 Please confirm for randomised controlled trials all versions of the clinical protocol are included in the submission. These will be published online as supplementary information.

Ramdomised controlled trial has been published previously [3] Van den Berghe G, Wouters P, Weekers F, Verwaest C, Bruyninckx F, Schetz M, et al. Intensive insulin therapy in critically ill patients. N Engl J Med 2001;345:1359–67. All protocol and consent forms were approved by the Institutional Review Board of the KU Leuven (ML1094, ML2707)

Supplementary Figures:

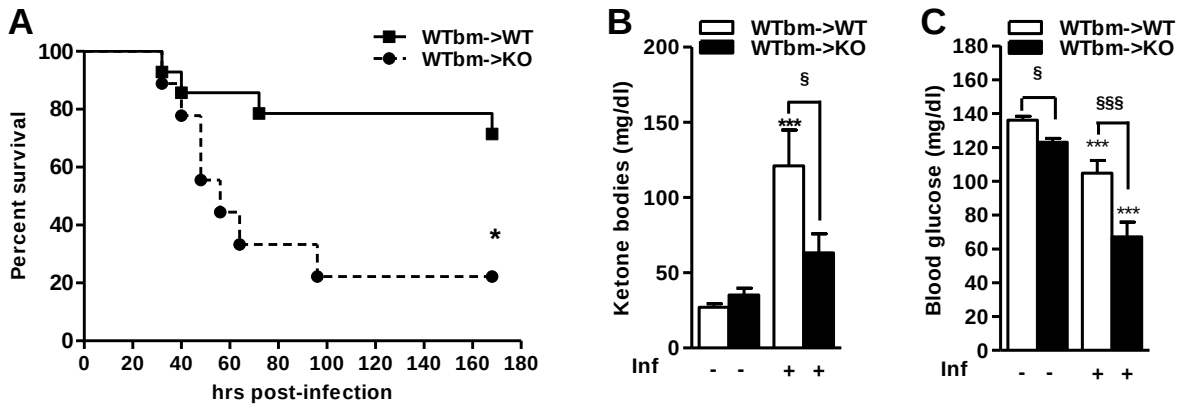

Supplementary Fig. 1: *Non-hematopoietic Pparα-deficiency enhances mortality and decreases plasma ketone bodies and glucose levels after bacterial infection.*

Pparα WT bone marrow (bm) was transplanted to lethally irradiated whole body *Pparα* WT (WTbm->WT) and *Pparα* KO (WTbm->KO) mice. After 8 weeks of recovery, *Pparα* WTbm->WT and *Pparα* WTbm->KO mice were injected (ip) with vehicle (PBS) (-) or *E.coli* ($4x10^8$ live bacteria) (Inf) (+). Survival was followed for 8 days after bacterial infection (n=12-15 mice /group) (A). Serum was collected 16hrs after bacterial infection and plasma ketone bodies (B) and blood glucose (C) concentrations were measured using a glucometer and an enzymatic test (n=8 mice/group). Statistical differences are indicated (Survival test: *Log-rank (Mantel-Cox) Test.* * $p<0.05$. *2way ANOVA*: *** $p<0.001$, ** $p<0.01$ and * $p<0.05$ for effect of infection; §§§ $p<0.001$; §§ $p<0.01$; § $p<0.05$ for effect of genotype; ns: non-significant).

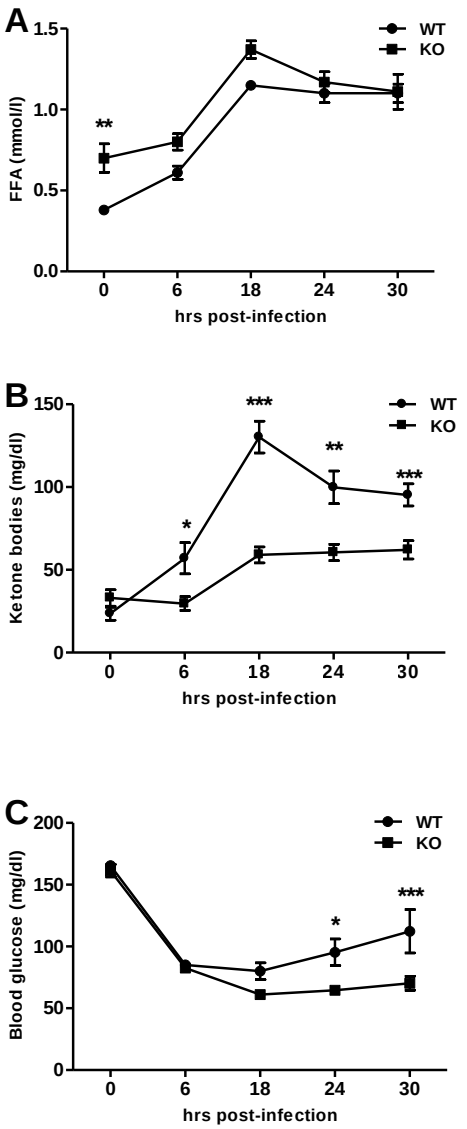

Supplementary Fig. 2: *Time course of the metabolic response of whole body Pparα-deficient mice to bacterial infection***.**

Whole body *Pparα* WT and KO mice were injected (ip) with *E.coli* ($4x10^8$ live bacteria). Serum was collected at different time point before (0) and at different time points after bacterial infection (6, 18, 24 and 30hrs) and FFA (A), ketone bodies (B), and blood glucose (C) concentrations were measured using a glucometer and enzymatic tests. Statistical differences are indicated (*2way ANOVA*: *** $p<0.001$, ** $p<0.01$ and * $p<0.05$ for effect of infection; §§§ $p<0.001$; §§ $p<0.01$; § $p<0.05$ for effect of genotype; ns: non-significant).

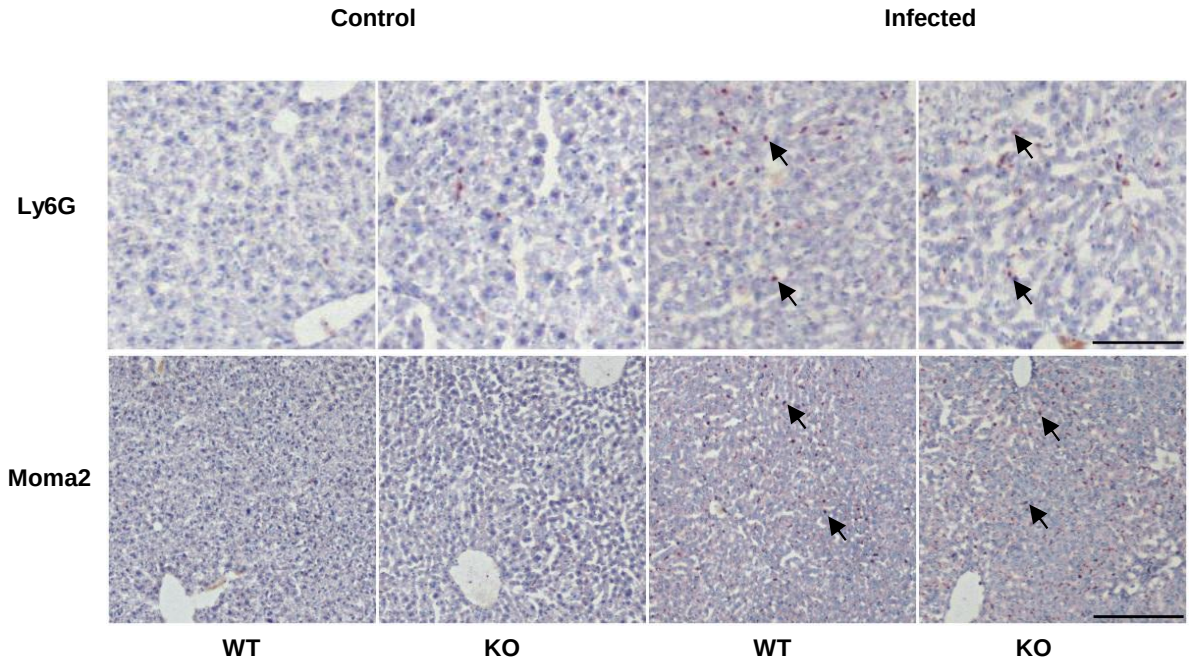

Supplementary Fig. 3: *Whole body Pparα-deficiency does not affect leukocyte recruitment in the liver after bacterial infection*

Whole body *Pparα* WT and KO mice were injected (ip) with vehicle (PBS) (Control) or *E.coli* ($4x10^8$ live bacteria) (Infected). Livers were collected 16hrs after bacterial infection. Liver sections were stained with antibodies against Ly6G (top panel) and Moma2 (bottom panel). Cells expressing Ly6G or Moma2 are indicated by arrows (n= 8 mice/group) (Bar = 500μm).

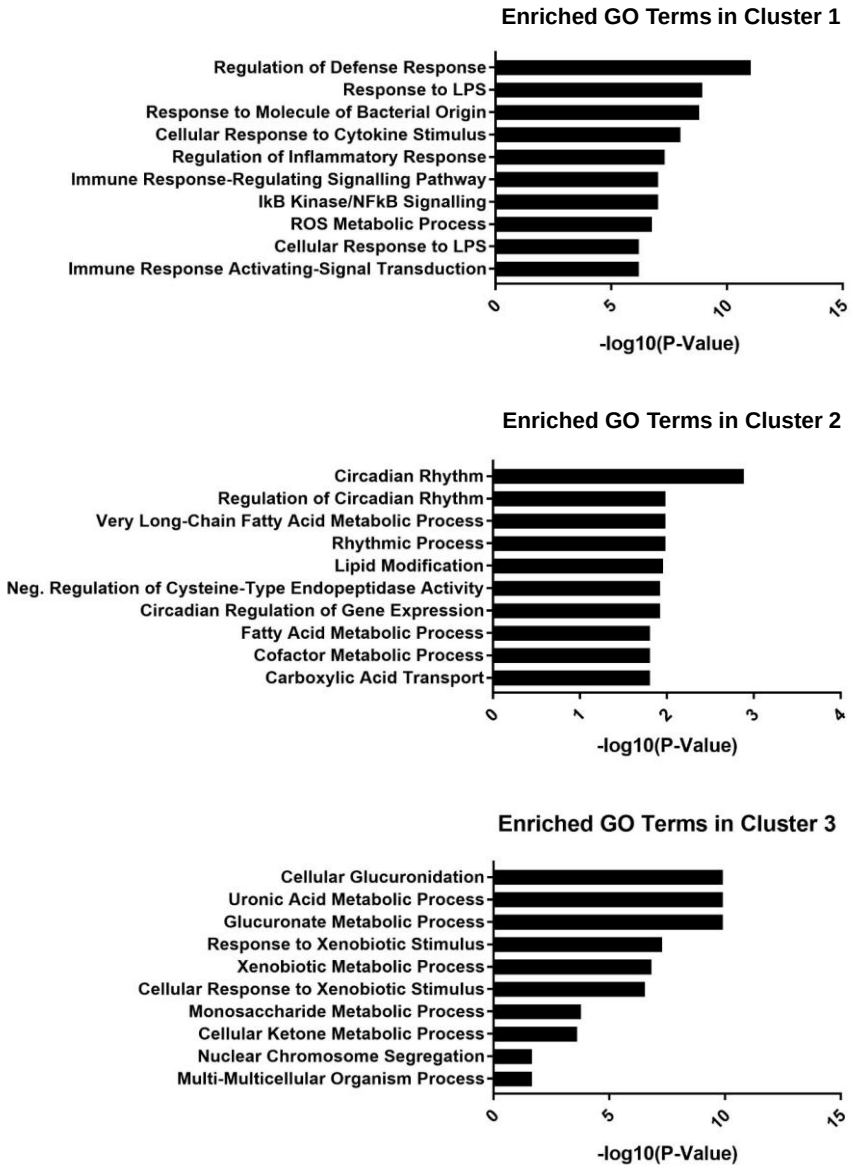

Supplementary Fig. 4: *Whole body Pparα-deficiency modulates the response to infection of metabolic and inflammatory gene expression pathways in the liver.*

Whole body *Pparα* WT and KO mice were injected (ip) with vehicle (PBS) (-) or *E.coli* ($4x10^8$ live bacteria) (Inf) (+). Livers were collected 16hrs after infection and microarray analysis were performed. GO terms enriched pathway analysis was performed on 3 clusters of genes displaying different response patterns in whole body *Pparα* WT versus *Pparα* KO.

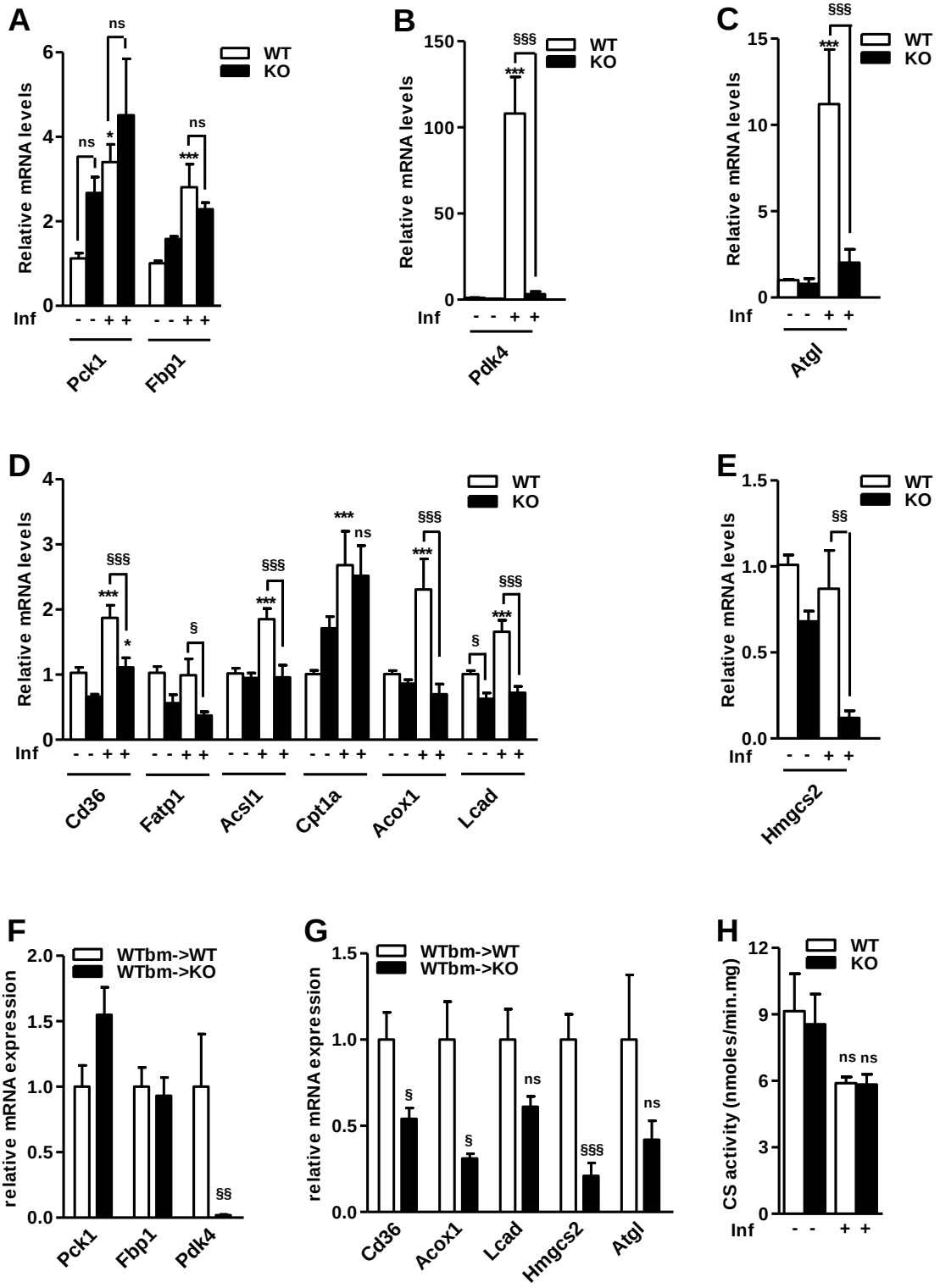
A
B
C
D
E
F
G
H
WT
KO
Relative mRNA levels
Inf
Pck1
Fbp1
Pdk4
Atgl
Cd36
Fatp1
Acsl1
Cpt1a
Acox1
Lcad
Hmgcs2
WTbm->WT
WTbm->KO
relative mRNA expression
CS activity (nmoles/min.mg)
ns
§§§
§§
§

Supplementary Fig. 5: *Influence of whole body and non-hematopoietic cell Pparα-deficiency on hepatic citrate synthase (CS) and glucose and lipid metabolic gene expression upon infection.*

Whole body *Pparα* WT and KO mice, *Pparα* WTbm->WT and WTbm->KO mice were injected (ip) with vehicle (PBS) (-) or *E.coli* ($4x10^8$ live bacteria) (Inf) (+). Livers were collected 16hrs after infection and hepatic mRNA levels of genes involved in gluconeogenesis (A, F), glycolysis (B, F), TG hydrolysis, FA uptake and β-oxidation and ketogenesis (D, E, G) were analysed using RT-Q-PCR. Citrate synthase activity was measured using enzymatic test (H) (n=7-8 mice/group). Statistical differences are indicated (*2way ANOVA*: *** $p<0.001$, ** $p<0.01$ and * $p<0.05$ for effect of infection; §§§ $p<0.001$; §§ $p<0.01$; § $p<0.05$ for effect of genotype; ns: non-significant).

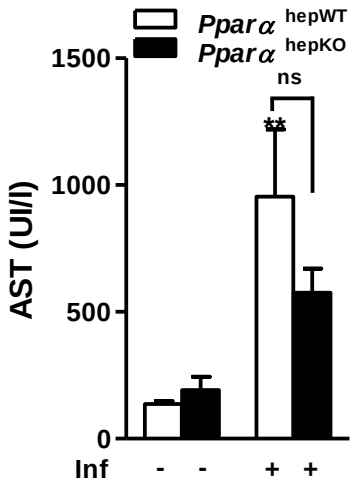

Supplementary Fig. 6: *Influence of hepatocyte-specific Pparα-deficiency on plasma AST levels upon bacterial infection.*

Pparα ^{hepWT} and *Pparα* ^{hepKO} mice were injected (ip) with vehicle (PBS) (-) or *E.coli* ($6x10^8$ live bacteria) (Inf) (+).Serum was collected 16hrs after bacterial infection and plasma AST levels were measured using an enzymatic assay as described in Materials and Methods (n=8 mice/group). Statistical differences are indicated (Survival test: *Log-rank (Mantel-Cox) Test.* * $p<0.05$. *2way ANOVA*: *** $p<0.001$, ** $p<0.01$ and * $p<0.05$ for effect of infection; §§§ $p<0.001$; §§ $p<0.01$; § $p<0.05$ for effect of genotype; ns: non-significant).

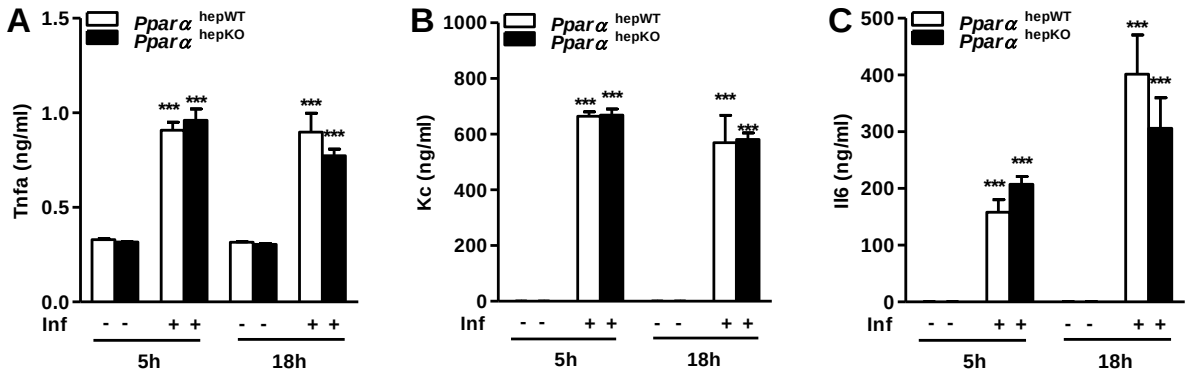

Supplementary Fig. 7: *Hepatocyte-specific Pparα-deficiency does not influence systemic inflammation markers upon bacterial infection.*

Pparα ^{hepWT} and *Pparα* ^{hepKO} mice were injected (ip) with vehicle (PBS) (-) or *E.coli* ($6x10^8$ live bacteria) (Inf) (+). Plasma was collected 5hrs and 16hrs after infection and Tnfa (A), Kc (B), and Il6 (C) were analyzed using Elisa tests. Statistical differences are indicated (*2way ANOVA*: *** $p<0.001$, ** $p<0.01$ and * $p<0.05$ for effect of infection).

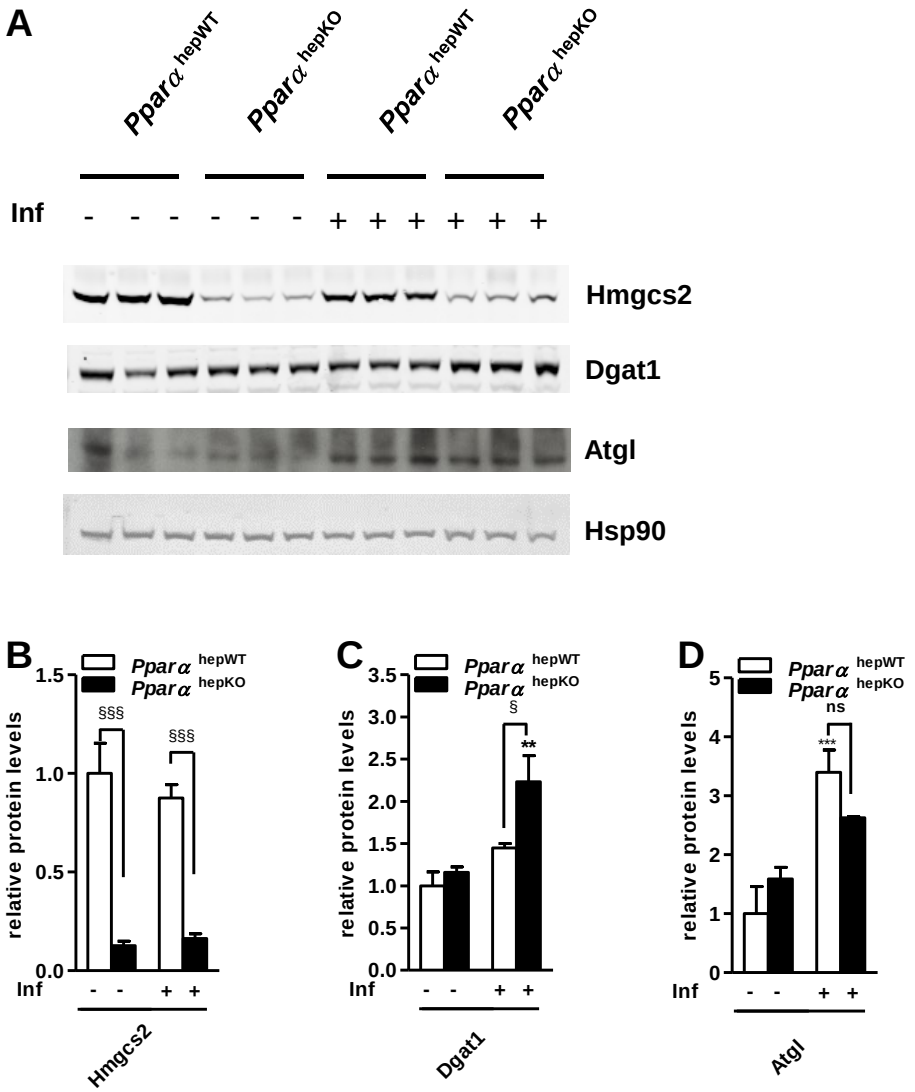

Supplementary Fig. 8: *Influence of hepatocyte-specific Pparα-deficiency on Hmgcs2, Dgat1 and Atgl protein levels in livers of infected and non-infected mice.*
Pparα ^{hepWT} and *Pparα* ^{hepKO} mice were injected (ip) with vehicle (PBS) (-) or *E.coli* ($6x10^8$ live bacteria) (Inf) (+). Livers were collected 16hrs after infection and hepatic Hmgcs2 (A, B), Dgat1 (A, C), Atgl (A, D) and Hsp90 (A) protein levels assessed using western-blot analysis and normalized to Hsp90 protein levels (B, C, D). (n=6, 2 pooled samples per each well). Statistical differences are indicated (*2way ANOVA*: *** $p<0.001$, ** $p<0.01$ and * $p<0.05$ for effect of infection; §§§ $p<0.001$; §§ $p<0.01$; § $p<0.05$ for effect of genotype; ns: non-significant).

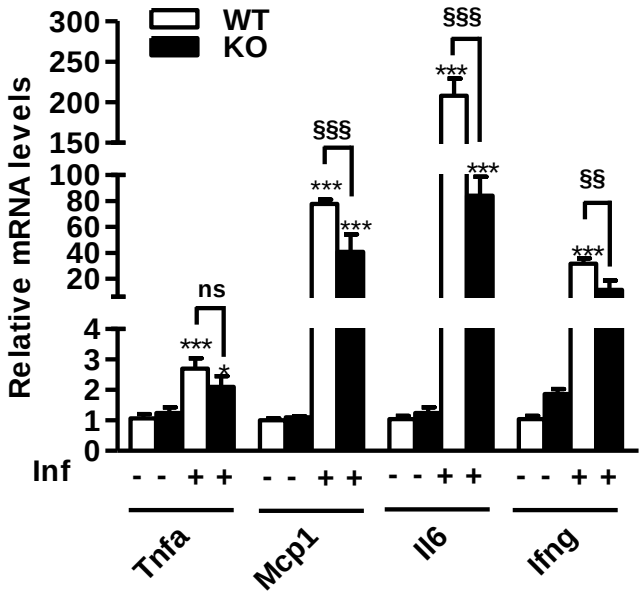

Supplementary Fig. 9: *Whole body Pparα-deficiency decreases the inflammatory response in the spleen of infected mice.*

Whole body *Pparα* WT and KO mice were injected (ip) with vehicle (PBS) (-) or *E.coli* ($4x10^8$ live bacteria) (Inf) (+). Spleens were collected 16hrs after bacterial infection and mRNA levels of genes involved in inflammation were analysed using RT-Q-PCR (n=7-8 mice/group). Statistical differences are indicated (*2way ANOVA*: *** $p<0.001$, ** $p<0.01$ and * $p<0.05$ for effect of infection; §§§ $p<0.001$; §§ $p<0.01$; § $p<0.05$ for effect of genotype; ns: non-significant).

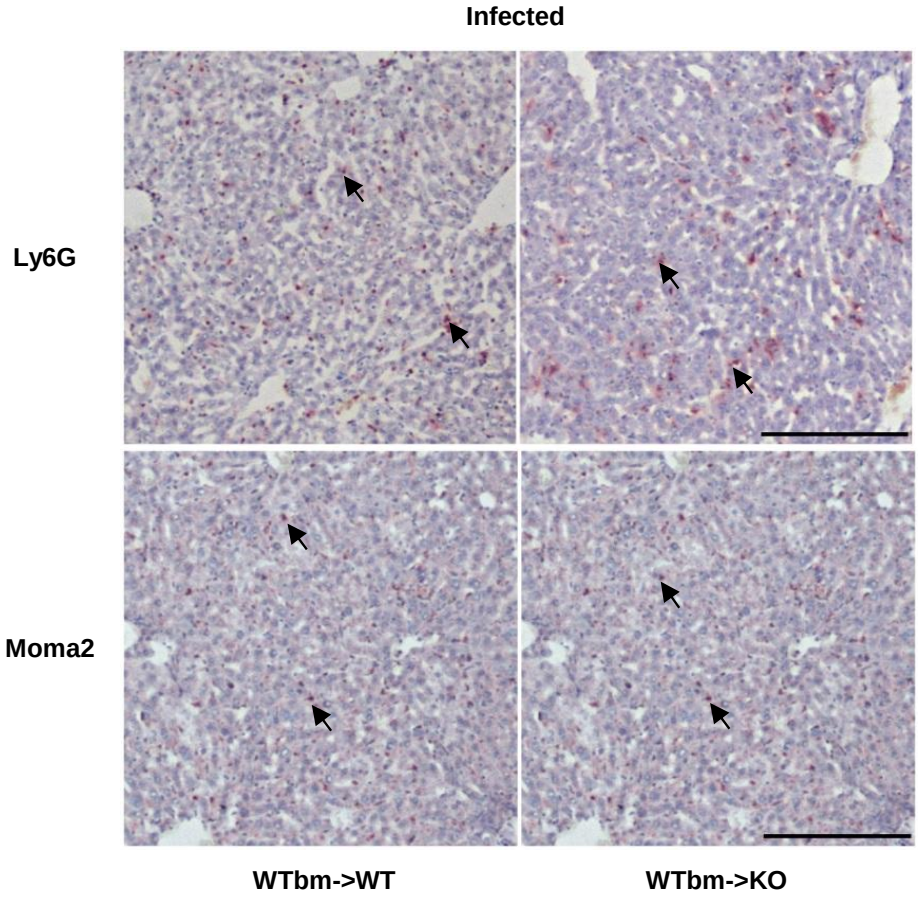

Supplementary Fig. 10: *Pparα-deficiency in non-hematopoietic cells does not affect hepatic leucocyte recruitment upon bacterial infection.*

Pparα WTbm->WT and WTbm->KO mice were injected (ip) with *E.coli* ($4x10^8$ live bacteria) (Infected). Livers were collected 16hrs after infection and liver sections were stained with antibodies against Ly6G (top panel) and Moma2 (bottom panel). Cells expressing Ly6G or Moma2 are indicated by arrows (n=7-8 mice/group) (Bar = 500μm).

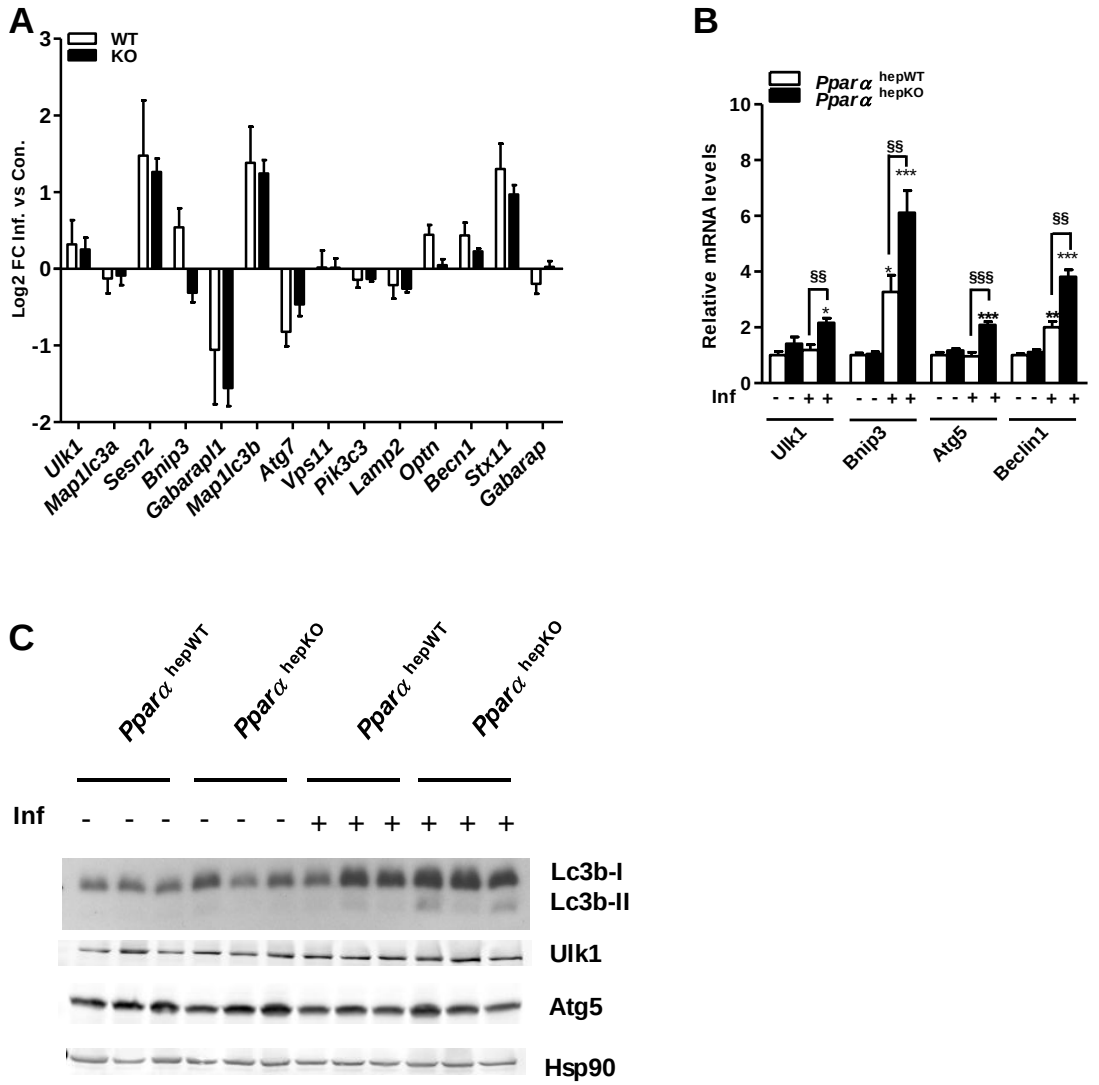

Supplementary Fig. 11: *Influence of whole body and hepatocyte-specific Pparα-deficiency on markers of autophagy upon bacterial infection.*

Whole body *Pparα* WT and *Pparα* KO mice, *Pparα* ^{hepWT} and hepatocyte-specific *Pparα* ^{hepKO} mice were injected (ip) with vehicle (PBS) (-) or *E.coli* (4-6x10^8 live bacteria) (Inf) (+). Livers were collected 16hrs after infection and microarray analysis was performed in whole body *Pparα* WT and *Pparα* KO liver RNA and autophagy pathway gene expression levels compared in infected vs non-infected mouse liver (A), Analysis of mRNA (B) and protein (C) expression levels of autophagy markers was performed on *Pparα* ^{hepWT} and *Pparα* ^{hepKO} livers using RT-Q-PCR and western-blot analysis, respectively. Statistical differences are indicated (*2way ANOVA*: *** $p<0.001$, ** $p<0.01$ and * $p<0.05$ for effect of infection; §§§ $p<0.001$; §§ $p<0.01$; § $p<0.05$ for effect of genotype; ns: non-significant).

Supplementary Table

Supplementary Table 1: *Baseline and outcome variables of studied critically ill patients and healthy volunteers.*

	Critically ill patients N=46	Healthy Controls N=20
Demographic data		
Male sex – no. (%)	29 (63)	13 (65)
Age – yr (mean ± SE)	69.8 ± 1.7	68.9 ± 2.9
BMI – Kg/m^2 (mean ± SE)	24.6 ± 0.5	25.1 ± 0.6
Comorbidity variables		
Malignancy no. (%)	15 (33)	
Diabetes no. (%)	4 (9)	
APACHE II score – median [IQR]	12 [10-19]	
Reason for admission or type of surgery (no.)		
Complicated abdominal surgery	7	
Complicated cardiothoracic surgery	28	
Multiple trauma and cerebral injury	7	
Other	4	
Outcome variables		
Bacteremia (no.) (%)	13 (28)	
Days in ICU (median [IQR])	12 [6-36]	
Cause of ICU death (no.)		
Acute hemodynamic collapse	4	
MOF with a proven septic focus	23	
MOF with SIRS	15	
Severe brain damage	4	

Table 1: Baseline and outcome variables of studied critically ill patients and healthy volunteers. BMI, body mass index; APACHE II score, Acute Physiology and Chronic Health Evaluation II APACHE II score reflecting severity of illness, with higher values indicating more severe illness, ranging from 0 to 71; ICU, intensive care unit; MOF multiple organ failure; SIRS, systemic inflammatory response syndrome.

Bibliography

[1] Montagner A, Polizzi A, Fouché E, Ducheix S, Lippi Y, Lasserre F, et al. Liver PPARα is crucial for whole-body fatty acid homeostasis and is protective against NAFLD. Gut 2016;65:1202–14. doi:10.1136/gutjnl-2015-310798.

[2] van den Berghe G, Wouters P, Weekers F, Verwaest C, Bruyninckx F, Schetz M, et al. Intensive insulin therapy in critically ill patients. N Engl J Med 2001;345:1359–67. doi:10.1056/NEJMoa011300.

[3] Biddinger SB, Hernandez-Ono A, Rask-Madsen C, Haas JT, Alemán JO, Suzuki R, et al. Hepatic insulin resistance is sufficient to produce dyslipidemia and susceptibility to atherosclerosis. Cell Metab 2008;7:125–34. doi:10.1016/j.cmet.2007.11.013.